A density functional theory study of two-dimensional bismuth selenite: layer-dependent electronic, transport and optical properties with spin-orbit coupling†

Yao Wang, [1,2*] Jinsen Zhang,[1*] Xuanlin Zhang,[4] Chenqiang Hua, [3,a)] Yunhao Lu,[4] and Xinyong Tao[1]

AFFILIATIONS

[1] College of Materials Science and Engineering, Zhejiang University of Technology, Hangzhou, 310014, China

[2] Moganshan Research Institute at Deqing County Zhejiang University of Technology, Huzhou, 313000, China

[3] Hangzhou International Innovation Institute, Beihang University, Hangzhou 311115, China

[4] School of Physics, Zhejiang University, Hangzhou 310027, China

[*]These authors contributed equally to this work.

[a)] **Author to whom correspondence should be addressed:** huachenqiang@buaa.edu.cn.

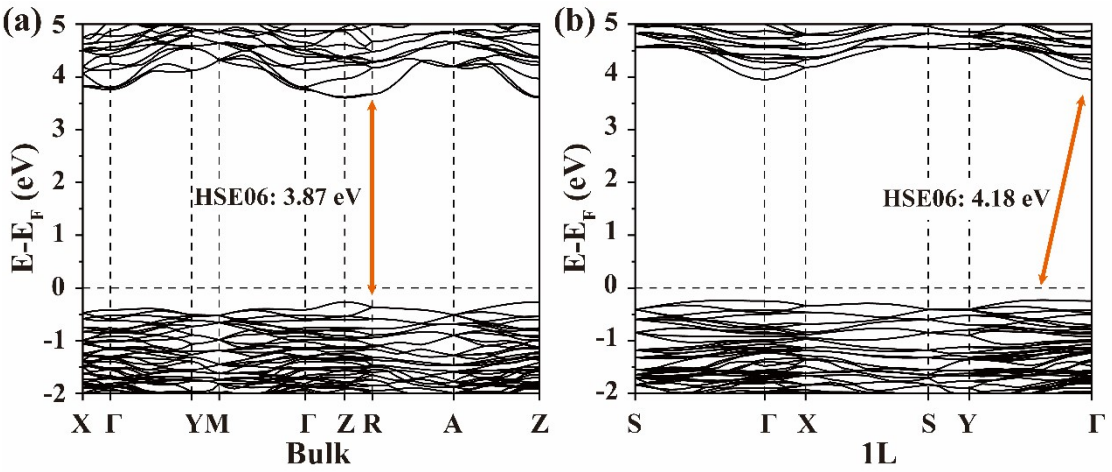

FIG. S1. Electronic structures of (a) bulk and (b) 1L Bi_2SeO_5 calculated with HSE06 functional.

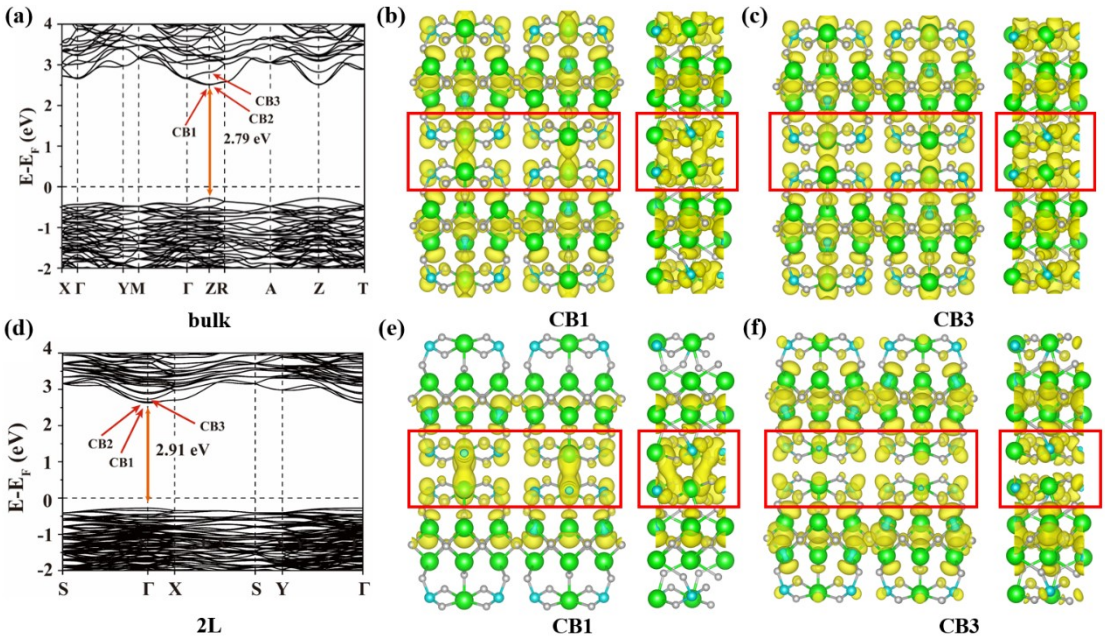

FIG. S2. (a, d) Electronic structures of bulk/2L Bi_2SeO_5. CB1, CB2 and CB3 are marked. Spatial distribution of wavefunction for the lowest CBs using an isosurface of 0.0008 eÅ^{-3} for bulk (b, c) and 2L (e, f) Bi_2SeO_5. For CB1, it is obvious to see that the interlayer charge distribution mimics the bonding-like behavior while antibonding-like for CB3. Besides, the perpendicular charge distribution always mixes some in-plane components, indicating the contribution of in-plane *p* orbitals.

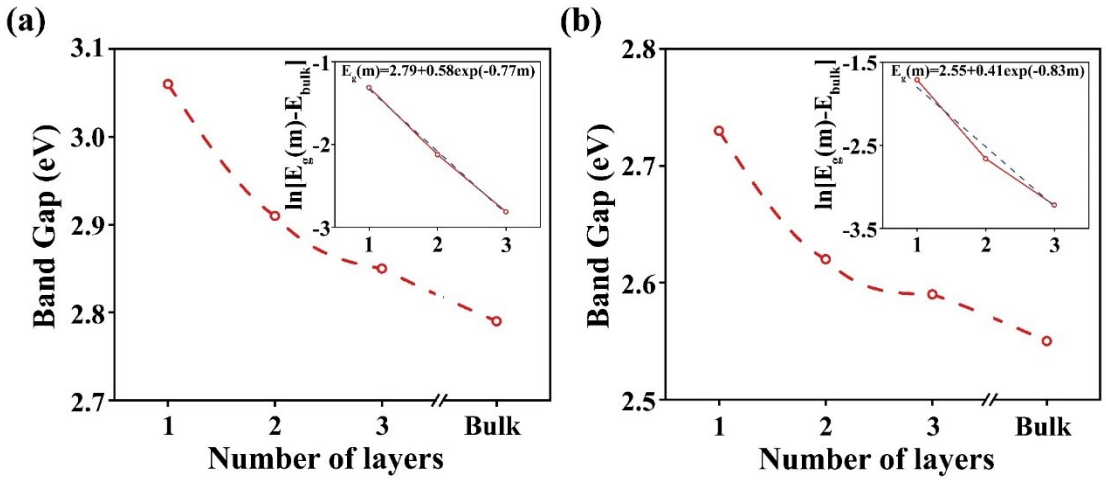

FIG. S3. The variation of bandgap $E_g(m)$ as a function of layer number m. Inset: The blue dash line indicates the linear fitting. For (a), SOC is not considered while for (b), SOC is included.

Note 1. The quantum confinement effect of 2D Bi_2SeO_5.

To qualitatively explore the quantum confinement effect, we calculate the relationship between the bandgap (E_g) and the layer number (m). As shown in **Fig. S3-inset**, an obvious linear dependence between $\ln[E_g(m)-E_g(bulk)]$ and m can be observed. Such behavior indicates that E_g versus m follows the equation below,

$$E_g(m) = E(bulk) + \alpha \exp(-\beta m). \quad (1)$$

where α and β are the characteristic parameters. The fitted curves are shown in **Fig. S3,** without considering SOC, the values of α and β are 0.58 and 0.77, respectively. When SOC is taken into account, the values of α and β are 0.41 and 0.83, respectively. This indicates that SOC plays a crucial role in the bandgap. With the above expression, it is convenient to predict the bandgap of multilayer Bi_2SeO_5 without the detailed calculation, which can accelerate the selection of 2D Bi_2SeO_5 with specific bandgap.

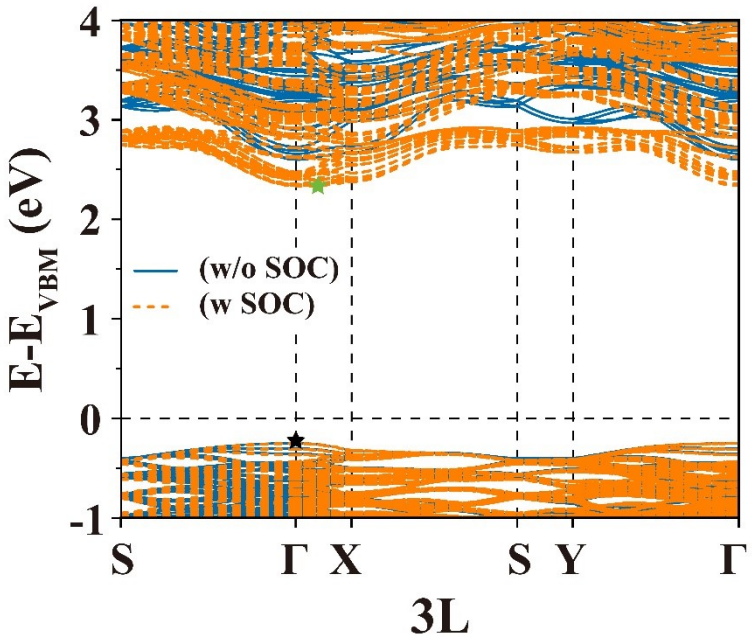

FIG. S4. Electronic band structure of 3L Bi_2SeO_5 with SOC (orange dashed lines). For easy comparison, we plot the bands without SOC together (blue solid lines). Green and black pentagrams represent CBM and VBM, respectively.

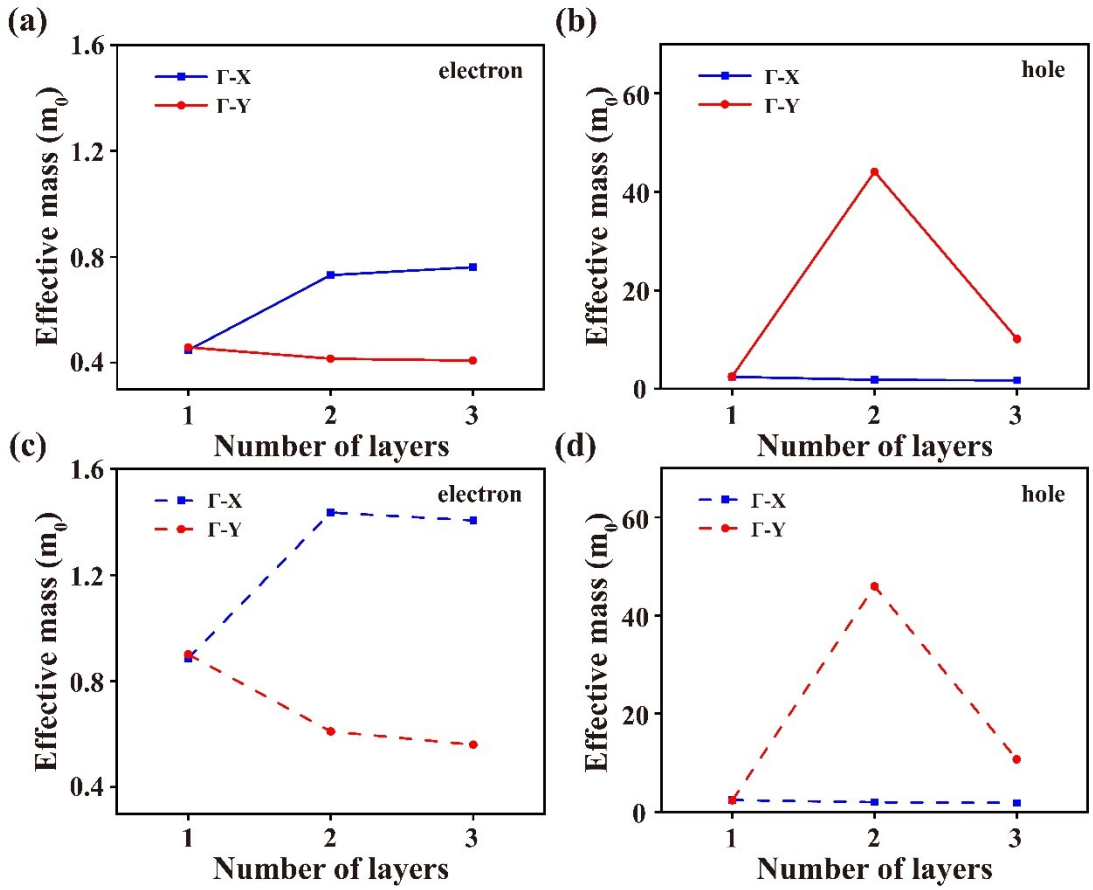

FIG. S5. Effective mass of (a, c) electrons and (b, d) holes along the Γ-X (blue) and Γ-Y (red) directions versus the number of layers. SOC is included for (c, d) with dashed lines.

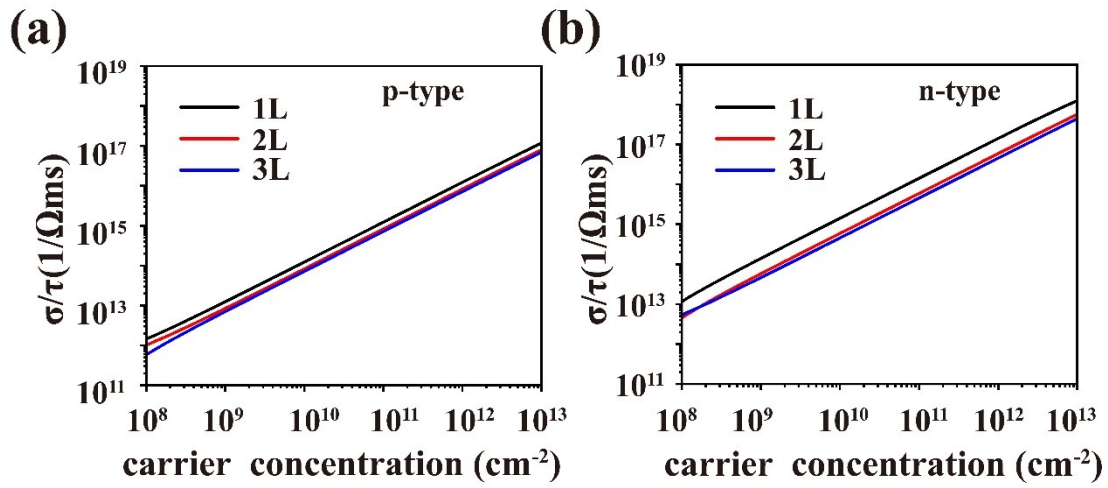

FIG. S6. The variation of (a-b) σ/τ with different doping concentration at 300 K for 2D Bi_2SeO_5.

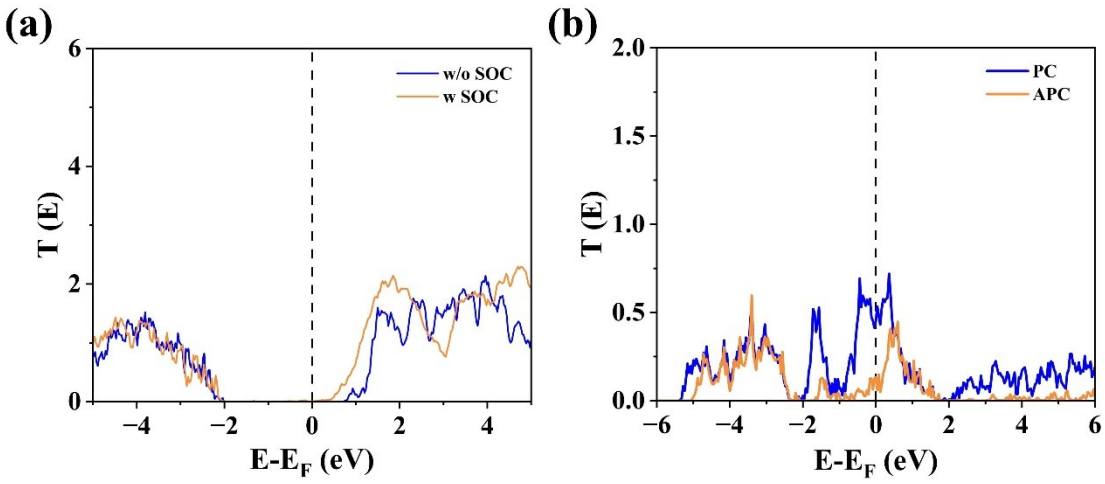

FIG. S7. (a) Transmission spectra of the Al/2L Bi_2SeO_5/Al device. (b) Transmission spectra of the FeS_2/2L Bi_2SeO_5/FeS_2 MTJ.

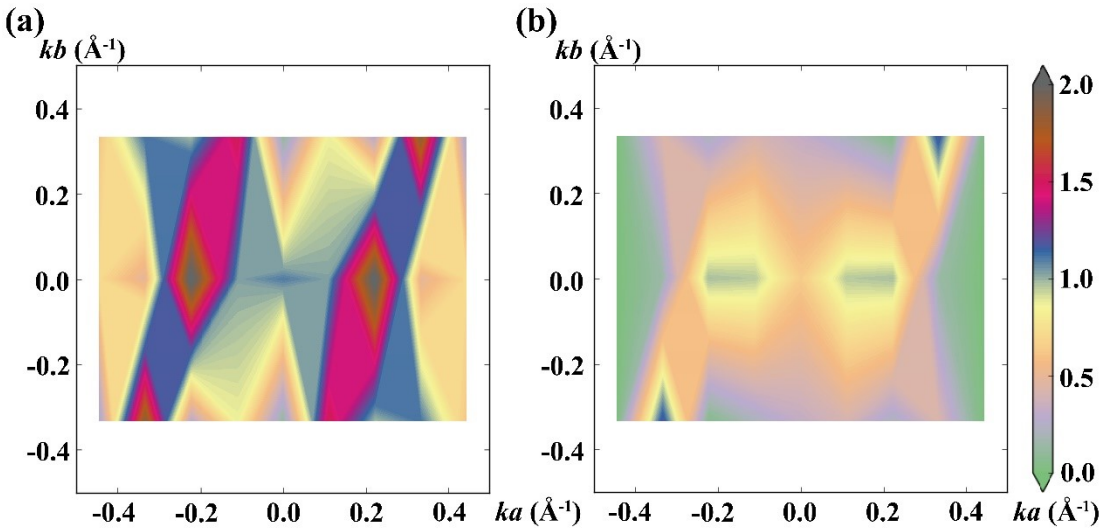

FIG. S8. *k*-resolved transmission coefficients for the FeS_2/1L Bi_2SeO_5/FeS_2 MTJ for the (a) PC and (b) APC states. E = 0 eV.

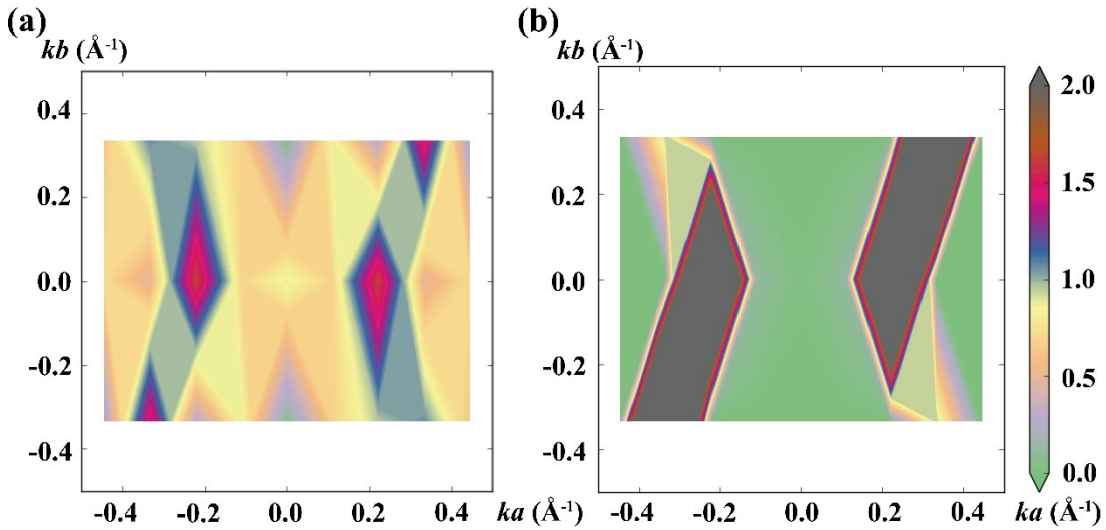

FIG. S9. *k*-resolved transmission coefficients for the FeS_2/2L Bi_2SeO_5/FeS_2 MTJ for the (a) PC and (b) APC states. $E = 0$ eV.

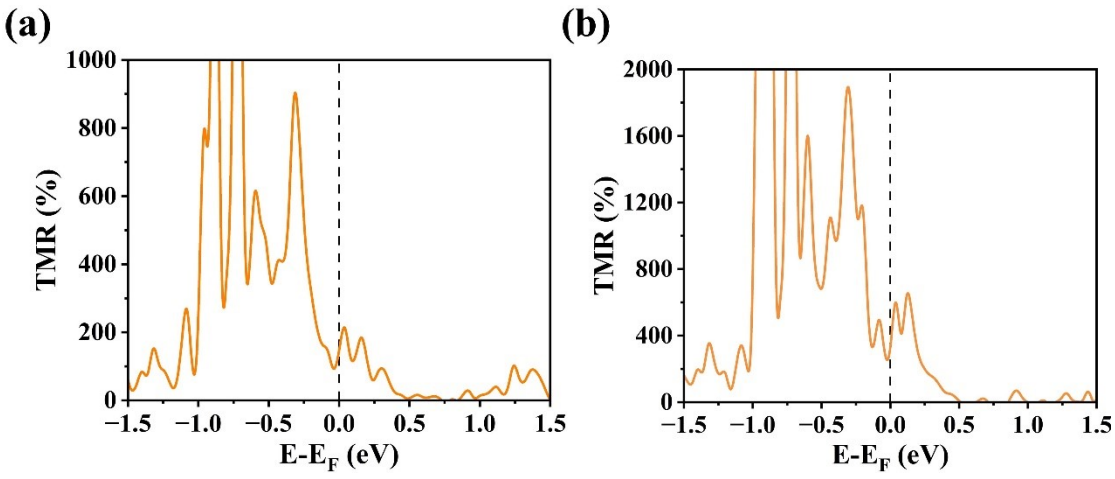

FIG. S10. TMR as a function of chemical potential (*E*) for (a) FeS_2/1L Bi_2SeO_5/FeS_2 and (b) FeS_2/2L Bi_2SeO_5/FeS_2 MTJs.

TABLE S1. Lattice constants and volume of bulk Bi_2SeO_5 calculated by using different computational methods.

System	a (Å)	b (Å)	c (Å)	V (Å^3)
Exp.[1]	11.44	16.28	5.49	1022.48
PBE[2]	11.64	16.68	5.57	1081.444
LDA[3]	11.09	16.12	5.43	970.7254
DFT-D2[4]	11.41	16.47	5.52	1037.333
DFT-D3[5]	11.49	16.52	5.55	1053.472
DFT-D3[6]	11.37	16.41	5.52	1029.931
DFT-D4[7]	11.65	16.69	5.57	1083.022
TS[8]	11.53	16.58	5.56	1062.891
TS/HI[9,10]	11.42	16.47	5.53	1040.123
MBD@rSC[11,12]	11.46	16.50	5.54	1047.559
MBD@rSC/FI[13,14]	11.64	16.68	5.57	1081.444
dDsC[15,16]	11.38	16.43	5.52	1032.093
DFT-ulg[17]	11.43	16.48	5.54	1043.55
vdW-DF[18]	11.71	16.80	5.63	1107.579
vdW-DF2[19]	11.68	16.87	5.66	1115.255
optPBE-vdW[20]	11.51	16.57	5.57	1062.314
optB88-vdW[20]	11.37	16.44	5.54	1035.552
optB86b-vdW[21]	11.33	16.37	5.52	1023.806
rev-vdW-DF2[22]	11.35	16.40	5.53	1029.354
vdW-DF-cx[23]	11.28	16.31	5.50	1011.872
rVV10[24]	11.23	16.32	5.52	1011.67
SCAN+rVV10[25]	11.21	16.18	5.46	990.3228

TABLE S2. Relative differences between DFT and experimental results (unit: %). A_0, b_0, c_0 and V_0 are the lattice constants and volume measured in the experiment.

System	$(a - a_0)/a_0$	$(b - b_0)/b_0$	$(c - c_0)/c_0$	$(V - V_0)/V_0$
DFT-D3	-0.61	0.80	0.55	0.73
dDsC	-0.52	0.92	0.55	0.94
optB88-vdW	-0.61	0.98	0.91	1.28
optB86b-vdW	-0.96	0.55	0.55	0.13
rev-vdW-DF2	-0.79	0.74	0.73	0.67

REFERENCES

[1]C. Zhang, T. Tu, J. Wang, Y. Zhu, C. Tan, L. Chen, M. Wu, R. Zhu, Y. Liu, H. Fu, J. Yu, Y. Zhang, X. Cong, X. Zhou, J. Zhao, T. Li, Z. Liao, X. Wu, K. Lai, B. Yan, P. Gao, Q. Huang, H. Xu, H. Hu, H. Liu, J. Yin, and H. Peng, Nat. Mater. **22**, 832 (2023).

[2]J. P. Perdew, K. Burke, and M. Ernzerhof, Phys. Rev. Lett. **77**, 3865 (1996).

[3]P. A. M. Dirac, Math. Proc. Cambridge Philos. Soc. **26**, 376 (1930).

[4]S. Grimme, J Comput. Chem. **27**, 1787 (2006).

[5]S. Grimme, J. Antony, S. Ehrlich, and H. Krieg, J. Chem. Phys. **132**, 154104 (2010).

[6]S. Grimme, S. Ehrlich, and L. Goerigk, J Comput. Chem. **32**, 1456 (2011).

[7]E. Caldeweyher, S. Ehlert, A. Hansen, H. Neugebauer, S. Spicher, C. Bannwarth, and S. Grimme, J. Chem. Phys. **150**, 154112 (2019).

[8]A. Tkatchenko and M. Scheffler, Phys. Rev. Lett. **102**, 073005 (2009).

[9]T. Bučko, S. Lebègue, J. G. Ángyán, and J. Hafner, J. Chem. Phys. **141**, 034114 (2014).

[10]T. Bučko, S. Lebègue, J. Hafner, and J. G. Ángyán, J. Chem. Phys. **9**, 4293 (2013).

[11]A. Ambrosetti, A. M. Reilly, R. A. DiStasio, Jr., and A. Tkatchenko, J. Chem. Phys. **140**, 18A508 (2014).

[12]A. Tkatchenko, R. A. DiStasio, R. Car, and M. Scheffler, Phys. Rev. Lett. **108**, 236402 (2012).

[13]T. Gould and T. Bučko, J. Chem. Phys. **12**, 3603 (2016).

[14]T. Gould, S. Lebègue, J. G. Ángyán, and T. Bučko, J. Chem. Phys. **12**, 5920 (2016).

[15]S. N. Steinmann and C. Corminboeuf, J. Chem. Phys. **134**, 044117 (2011).

[16]S. N. Steinmann and C. Corminboeuf, J. Chem. Phys. **7**, 3567 (2011).

[17]H. Kim, J.-M. Choi, and W. A. Goddard, III, J. Phys. Chem. Lett. **3**, 360 (2012).

[18]M. Dion, H. Rydberg, E. Schröder, D. C. Langreth, and B. I. Lundqvist, Phys. Rev. Lett. **92**, 246401 (2004).

[19]K. Lee, É. D. Murray, L. Kong, B. I. Lundqvist, and D. C. Langreth, Phys. Rev. B **82**, 081101 (2010).

[20]J. Klimeš, D. R. Bowler, and A. Michaelides, Journal of Physics: Condensed Matter **22**, 022201 (2010).

[21]J. Klimeš, D. R. Bowler, and A. Michaelides, Phys. Rev. B **83**, 195131 (2011).

[22]I. Hamada, Phys. Rev. B **89**, 121103 (2014).

[23]K. Berland and P. Hyldgaard, Phys. Rev. B **89**, 035412 (2014).

[24]R. Sabatini, T. Gorni, and S. de Gironcoli, Phys. Rev. B **87**, 041108 (2013).

[25]H. Peng, Z.-H. Yang, J. P. Perdew, and J. Sun, Phys. Rev. X **6**, 041005 (2016).